DEVELOPMENT AND ANALYTICAL VALIDATION OF A RADIOIMMUNOASSAY FOR THE MEASUREMENT OF TRYPSIN-LIKE IMMUNOREACTIVITY IN FERRET SERUM

A Thesis

by

CORY SETH BRIDGES

Submitted to the Office of Graduate and Professional Studies of
Texas A&M University
in partial fulfillment of the requirements for the degree of

MASTER OF SCIENCE

Chair of Committee,	Joerg M. Steiner
Co-Chair of Committee,	Jan S. Suchodolski
Committee Members,	Jonathan A. Lidbury
	Barbara J. Gastel
Head of Department,	Jonathan M. Levine

May 2017

Major Subject: Biomedical Sciences

ABSTRACT

Ferrets are valuable animal models for the study of many human diseases. Cystic fibrosis (CF) and pancreatitis are two such human diseases that could benefit from a ferret model. The pancreatic disease processes that occur in the ferret animal model may allow researchers to investigate the pathophysiology of these diseases and help to develop new therapeutics for them. Trypsin-like immunoreactivity (TLI) is a non-invasive diagnostic tool used to assess exocrine pancreatic function in humans, dogs, and cats. Therefore, the major objective of this project was to purify trypsin from ferret pancreas and to set up and analytically validate a radioimmunoassay (RIA) for the measurement of TLI in ferret serum.

Ferrets euthanized for unrelated projects had their pancreata removed and frozen at -80°C for further purification. Ferret trypsin was purified from pancreatic tissue and antiserum against ferret trypsin was raised in rabbits. Tracer was produced by the chloramine-T method. A radioimmunoassay was set up and analytically validated by determination of dilutional parallelism, spiking recovery, intra-assay variability, inter-assay variability, and sensitivity. A reference interval was established from 35 healthy ferret serum samples. A small group of ferrets with acute pancreatitis (AP; n = 3) and healthy controls (HC; n = 4) were analyzed by the new TLI RIA.

We conclude that the ferret TLI RIA is analytically sensitive, accurate, precise, reproducible, and sufficiently linear for the measurement of TLI in serum samples from ferrets. All AP ferrets had higher serum TLI concentrations than HC ferrets, although the

sample size was small. Further studies evaluating the usefulness of measuring serum ferret TLI concentrations in animal models with AP and CF are underway.

CONTRIBUTORS AND FUNDING SOURCES

Contributors

This work was supervised by a thesis committee consisting of Professors Joerg M. Steiner, Jan S. Suchodolski, Jonathan A. Lidbury, and Barbara J. Gastel and Head of the Department of Small Animal Clinical Sciences Jonathan M. Levine.

Ferret pancreatic tissue and lipase activity data were provided by Dr. John F. Engelhardt and colleagues from the University of Iowa Carver College of Medicine.

Purification and characterization of ferret trypsin were assisted by Pamela Miller of the Gastrointestinal Laboratory. All other work conducted for the thesis was completed by the student independently.

Funding Sources

There are no outside funding contributions to acknowledge related to the research and compilation of this document.

NOMENCLATURE

AP	Acute pancreatitis
CCK	Cholecystokinin
CF	Cystic fibrosis
CFTR	Cystic fibrosis conductance regulator
CPM	Counts per minute
EPI	Exocrine pancreatic insufficiency
IRT	Immunoreactive trypsinogen test
LLOD	Lower limit of detection
RIA	Radioimmunoassay
TLI	Trypsin-like immunoreactivity

TABLE OF CONTENTS

Page

LIST OF FIGURES

Page

LIST OF TABLES

Page

1. INTRODUCTION

1.1 Radioimmunoassays for the measurement of trypsin-like immunoreactivity in serum

Human trypsin was first purified from pancreatic tissue by Travis and Roberts [1] in 1969, and the first radioimmunoassay (RIA) for the measurement of human trypsin-like immunoreactivity (TLI) was developed by Geokas and Brodrick [2] in 1979. The TLI RIA measures not only trypsin, but also its zymogen trypsinogen. Trypsinogen is produced only in the acinar cells of the pancreas, so measurement of this inactive precursor provides a minimally-invasive tool for the assessment of exocrine pancreatic function. Also, serum concentrations of trypsin and trypsinogen and therefore TLI may increase when there is pancreatic inflammation [3].

In humans, newborn screening for cystic fibrosis (CF) includes testing for TLI concentration in serum (or dried blood spots). Infants with high TLI concentrations are promptly retested in order to reconfirm CF as well as to continue to evaluate them for CF. Over time, pancreatic exocrine cell destruction leads to decreased secretion of pancreatic enzymes and serum TLI concentrations that are characteristic of pancreatic insufficiency. In turn, CF patients with pancreatic insufficiency require lifelong enzyme supplementation [4].

To date, there are three other species besides humans for which an immunoassay for the measurement of TLI in serum has been developed: dogs, cats, and horses [5,6,7]. Despite ferrets being a well-known animal model for human CF and a potential animal

model for human pancreatitis, to the author's knowledge, there is no immunoassay available for the measurement of serum TLI concentrations in ferret (*Mustela putorius furo*) serum [8].

1.2 Cystic fibrosis

Cystic fibrosis (CF) is an incurable genetic disease caused by mutations in the CF transmembrane conductance regulator (CFTR) gene. Historically, CF was noted to primarily affect Caucasians, but CF has now been reported in patients of all ethnicities [9]. In the United States, more than 1,000 patients are newly diagnosed every year. Also, newborn screening for CF has been responsible for 60 percent of new diagnoses in 2013 [10]. Infants are screened for CF by an immunoreactive trypsinogen test, which measures the concentration of trypsinogen in the blood [4]. Also, a DNA-based test for the diagnosis of CF is commercially available and identifies greater than 90% of CFTR mutations. This may allow for greater personalized care of CF patients by identifying which clinical symptoms are most associated with a particular genotype [11]. The gold standard for the diagnosis of CF is an electrolyte test. This test measures chloride concentration in sweat after electrical stimulation of a sweat gland. If the chloride concentration is greater than 60 mmol/L, the patient is considered CF positive [12].

There is no cure for CF, but medical advances have increased life expectancy and the median age of survival is now greater than 40 years in developed countries [10]. Although CF was once thought of as a pediatric disease in which patients do not live into adulthood, CF diagnosis and treatment has increased life expectancy drastically in the last 50 years. Newborn screening and early diagnosis allow patients to receive the

therapy and supplementation they need, before the manifestation of clinical signs. This, along with life-long medical treatment, has allowed many patients with CF to live relatively normal lives [13].

In the 85 years since CF was first described, one of the most important discoveries was how the CFTR gene mutation resulted in CF. The CTFR protein functions as a chloride and bicarbonate transporter in epithelial and blood cells and genetic mutations result in thick mucus, which blocks ducts and secretory cells. Since secretory cells are located throughout the body, CF is thought of as a multisystemic disease. CF affects upper and lower airways, exocrine pancreas, liver, reproductive tract, and gastrointestinal tract [14].

Lung disease is the most prominent clinical manifestation of CF. First, mucus obstructs the airways and submucosal glands. Next, the lungs are colonized with pathogenic bacteria because the lungs cannot be properly cleared, which leads to an inflammatory response to these bacteria [11]. This chronic respiratory infection may become so severe that a lung transplant may be required [15]. In fact, CF accounted for 15.4% of all adult lung transplants from January 2004 to June 2015 (n = 36,327) [16].

Although the lungs are the primary organ affected, the pancreas is one of the earliest affected organs [17]. Classic CF presents with sticky mucus and blocked pancreatic ducts. This leads to decreased amounts of pancreatic enzymes and zymogens being released into the small intestine. Without these enzymes, which are necessary to properly digest protein and fat, CF patients are often malnourished and have clinical signs of gastrointestinal disease, such as loose stools or diarrhea. The nutritional status of

CF patients is highly predictive of survival, and pancreatic enzyme therapy combined with a specialized diet can greatly increase longevity [18].

1.3 The exocrine pancreas in human patients with cystic fibrosis

In 1938, Dr. Dorothy Anderson first described necropsy findings in humans with cystic fibrosis (CF). She noted the fibrotic cysts formed within the pancreas and named the disease cystic fibrosis [19]. In 1989, genetic research of CF determined that a defective CFTR gene was responsible for CF [20]. This defective transport protein leads to impaired anion (Cl^- and HCO_3^-) transport into the proximal ducts of the pancreas. The decreased flow of secretions combined with a high protein concentration can lead to precipitation of secreted proteins. These proteins can obstruct intraluminal ducts and cause pancreatic destruction [21]. The degree of pancreatic insufficiency and its rate of progression are largely linked to genetic factors [17]. There are six classes of CTFR mutations, and the mutations can be placed into two groups based on the status of the exocrine pancreatic function. Classes I, II, III, and VI are homozygous or compound heterozygous for severe alleles and lead to pancreatic insufficiency, while classes IV and V are not associated with pancreatic insufficiency [22]. Most CF patients fall into the first group, with about 85% of patients requiring pancreatic enzyme supplementation by age 2 [13]. Without supplementation, these patients exhibit nutritional deficiencies, especially due to the malabsorption of protein, fat, and fat-soluble vitamins in the small intestine [23]. Although pancreatitis has been shown to have a low prevalence among CF patients, mild CF mutations (classes IV and V) are considered a risk factor for both mild acute and chronic pancreatitis [24].

1.4 Animal models for cystic fibrosis

Animal models are an important research tool for studying the mechanisms of many diseases. Animal models for cystic fibrosis (CF) were developed not long after the genetic mutation of the CFTR was characterized. Several animal models have been developed to study CF pathogenesis, including the mouse, rat, zebrafish, pig, and ferret [25,26]. Cystic fibrosis is a multisystemic disease that affects several organs and that is associated with various clinical signs. The diverse clinical nature of CF has called for a diverse set of animal models. Each of these animal models has advantages and disadvantages. For example, if CF researchers are interested in studying meconium ileus (MI), an intestinal obstruction that occurs in about 15%-20% of newborns with CF, the pig would be best used as a model because the CF pig shows a 100% incidence of MI at birth. There are also genetically modified CF pigs where CFTR expression has been restored in the intestine, which can serve as controls [27]. Development of these animal models creates more conduits to better understand CF pathogenesis and create improved therapeutic options for humans with CF.

1.5 Ferret animal model for cystic fibrosis

At first, most CF research utilizing animal models was done with mouse strains with a mutated CFTR gene. However, mouse models lack significant pancreatic and pulmonary pathology similar to that of larger mammals [28]. These shortcomings led to the development of different CTFR recessive animal models, including rats, pigs, and ferrets [27]. CFTR-knockout ferrets exhibit similar disease characteristics to humans, especially in the lungs and the exocrine pancreas. Along with a short gestation time and

sexual maturation at 4 to 6 months, the similar lung physiology makes the ferret model ideal for studying lung infections [29]. Other diseases that have been studied using ferret animal models include severe acute respiratory syndrome and influenza virus [30,31]. Similar to the lungs, the exocrine pancreas of the ferret is anatomically very similar to that of humans. CF ferrets have been shown to exhibit exocrine pancreatic insufficiency (EPI), paralleling that observed in human CF patients, where EPI is estimated to develop in 80%-90% of CF patients [14].

1.6 The exocrine pancreas in cystic fibrosis ferrets

Gastrointestinal disease in CFTR-knockout ferrets has been characterized by Xingshen Sun and colleagues [32]. They observed that CF ferrets exhibit progressive pancreatic disease after birth. Fecal elastase-1 concentrations and histology were used to determine the degree of pancreatic disease. Extensive fibrosis and loss of exocrine pancreatic function was observed in 11 of 13 CF ferrets in their study. This parallels humans with CF, in which 80%-90% of patients are known to be develop exocrine pancreatic insufficiency [33]. Interestingly, the two CF ferrets that had normal pancreatic function and histology were raised in the same environment as the other CF ferrets, suggesting that genetic factors play an important role in the severity of the disease [32]. Using the CF ferret as a model will allow researchers to evaluate genetic and environmental factors that determine disease severity as it relates to the exocrine pancreas in CF patients.

1.7 Acute pancreatitis

Pancreatitis, an inflammatory disease of the pancreas, is poorly understood and can be acute or chronic. In humans, the most common causes of pancreatitis are gallstones or alcohol consumption [34]. Chronic pancreatitis can be defined as a persistent and progressive inflammatory disease of the pancreas, while acute pancreatitis (AP) is a short-lived, inflammatory response of the pancreas that is corrected by an anti-inflammatory response [35,36]. Smoking and type 2 diabetes may increase the risk for acute pancreatitis [37]. In humans, serum amylase and lipase activities above three times the upper limit of the upper reference interval are one criterion for a potential diagnosis of AP [36].

Although the pathophysiology of AP is still not well understood, it is known that pancreatic duct obstruction and/or pancreatic cell damage leads to blockage of the release of pancreatic enzymes into the small intestine. As the disease progresses, an excess of enzymes, such as trypsin, accumulates in acinar cells and leads to acinar cell damage. Premature trypsin activation, most likely promoted by cathepsin B, results in autodigestion of pancreatic acinar cells [38]. Acinar cell injury then stimulates an inflammatory response. The release of cytokines and chemokines attracts inflammatory cells, resulting in continued pancreatic destruction. This can lead to necrotic changes in the pancreatic tissue and multiple organ dysfunction [39]. Animal models can give researchers a better understanding of the pathophysiology of pancreatitis and may lead to novel biomarkers and treatments [34].

1.8 Animal models of pancreatitis

In 1856, the first animal model for pancreatitis was established. This model was a rabbit model, where bile and olive oil were injected into the pancreatic duct. To date, various rodent models, both non-invasive and invasive, are the most widely used models due to their reproducibility and low-cost [34].

Non-invasive models of pancreatitis include hormone hyperstimulation and dietary modification, while invasive models include closing off a duodenal loop or ligating the pancreatic duct. For example, the secretagogue caerulein, a cholecystokinin (CCK) hormone analogue, stimulates pancreatic enzyme synthesis and secretion, and hyperstimulation through administration of caerulein may result in pancreatic cell damage. This model is relatively simple and easy to reproduce, while allowing investigation of pancreatic cell regeneration after cessation of secretagogue administration. Unfortunately, CCK hyperstimulation is not a known cause of AP in humans. Similarly, alcohol feeding does not induce AP in many animal models, even though it is one of the main causes of AP in humans [38]. There have been many studies attempting to combine and modify different strategies for inducing and studying AP in animal models to most closely resemble human AP, but every model is lacking in one way or another [34].

All animal models of AP lead to clinical signs of lethargy, vomiting, and abdominal pain while resulting in mild to severe pancreatitis. Current small animal models of pancreatitis include rodents, rabbits, possums, dogs, and cats [40]. As the pathophysiology of pancreatitis remains largely unknown, a diverse set of animal models

with different methods to induce pancreatitis can help solve different parts of the pancreatitis puzzle. Adding the ferret animal model may provide new insights into the pathophysiology of human pancreatitis.

1.9 Potential ferret model of pancreatitis

As noted previously, the pancreas of the ferret is anatomically and physiologically similar to that of humans. Therefore, ferrets may potentially serve as an animal model for human pancreatitis. The current mouse and rat pancreatitis models usually exhibit mild pancreatitis, and dogs are expensive to house compared to ferrets. Many of the procedures that are used to induce pancreatitis in other small mammals should be easily reproducible in the ferret [34]. Ferrets currently serve as animal models for several other diseases, including cystic fibrosis, severe acute respiratory syndrome (SARS), and influenza [32,30,31]. A RIA for the measurement of TLI in ferret serum would be an invaluable minimally-invasive tool to facilitate the establishment of a novel pancreatitis ferret model.

2. MATERIALS AND METHODS

2.1 Materials

Pancreata were collected from euthanized ferrets from various research projects by Dr. Engelhardt, Yaling Yi, and colleagues from the University of Iowa Carver College of Medicine and were placed into a 15 mL centrifuge tube (two pancreata per tube). The tubes were labeled with the identification number of both ferrets and shipped overnight on dry ice to the Gastrointestinal Laboratory at Texas A&M University. All chemicals used were purchased from Sigma-Aldrich, St. Louis, MO, USA. The following materials were also used:

^{125}Iodine	Perkin Elmer, Waltham, MA, USA
Bovine serum albumin	Pierce Chemical CO, Rockford, IL, USA
Coomassie brilliant blue G-250	Pierce Chemical CO, Rockford, IL, USA
Imperial protein stain	Pierce Chemical CO, Rockford, IL, USA
Mark 12	Invitrogen, Carlsbad, CA, USA
NuPAGE 12% Bis-Tris gel	Invitrogen, Carlsbad, CA, USA
NuPAGE LDS sample buffer	Invitrogen, Carlsbad, CA, USA
NuPAGE MOPS SDS running buffer	Invitrogen, Carlsbad, CA, USA
NuPAGE sample reducing agent	Invitrogen, Carlsbad, CA, USA
Precipitating solution (PPT)	MP Biomedicals, Santa Ana, CA, USA
Polyacrylamide	Bio-Rad Laboratories, Hercules, CA, USA
Rabbit carrier solution (RCS)	Sigma Chemicals, St. Louis, MO, USA

SeeBlue Plus2	Invitrogen, Carlsbad, CA, USA
Silver stain kit Pierce	Chemical CO, Rockford, IL, USA

2.1.1 Instruments and machines

2470 Automatic Gamma Counter Wizard^{2}®	Perkin Elmer, Waltham, MA, USA
ÄKTA basic & fraction collector Frac-900	GE Healthcare, Uppsala, Sweden
Benzamidine column	GE Healthcare, Uppsala, Sweden
Centrifuge 5810R	Eppendorf AG, Hamburg, Germany
Centrifuge Allegra® X-15R	Beckman Coulter, Brea, CA, USA
Centrifuge rotor F 34-6-38	Eppendorf AG, Hamburg, Germany
Centrifuge rotor A-4-81	Eppendorf AG, Hamburg, Germany
Centrifuge rotor SX4750A Aries™	Beckman Coulter, Brea, CA, USA
Gel Doc™ XR+ System	Bio-Rad Laboratories, Hercules, CA, USA
Incubator – Boekel Model 133000	Boekel Scientific, Feasterville, PA, USA
pH-meter – Orion Star A211	Thermo Scientific, Rockford, IL, USA
Pipetman® P-20, P-100, P-200, P-1000	Rainin, Woburn, MA, USA
Pipette E4XLS Multichannel P-300	Rainin, Woburn, MA, USA
Pipettes E4XLS P-20, P-100, P-300, P-1000	Rainin, Woburn, MA, USA
Pipette P-5000	Eppendorf Research, Germany
Polytron homogenizer, PT-MR2100	Kinematica AG, Switzerland
Power Ease 500 (for electrophoresis)	Invitrogen, Carlsbad, CA, USA
Sephacryl S-100 26 x 60 HR column	GE Healthcare, Uppsala, Sweden
Scale - Voyager Pro	Ohaus, Parsippany, NJ, USA

Scale - XS6002S	Mettler Toledo, Columbus, OH, USA
Spectrophotometer - Ultrospec 2000	GE Healthcare, Uppsala, Sweden
Standard stirrer	VWR, West Chester, PA, USA
VX-2500 multi-tube vortexer	Fisher Scientific, Pittsburgh, PA, USA

2.1.2 Disposable materials

Blue Max™ Jr. (polypropylene, 15 mL)	Falcon, Franklin Lakes, NJ, USA
Centrifuge tubes (polypropylene, 50 mL)	VWR, West Chester, PA, USA
Culture tubes (polypropylene, 12 x 75 mm)	VWR, West Chester, PA, USA
Culture tubes (polystyrene, 12 x 75 mm)	VWR, West Chester, PA, USA
Glass culture tubes (12 x 75 mm)	VWR, West Chester, PA, USA
Parafilm®	VWR, West Chester, PA, USA
Magnetic micro-stir bar	VWR, West Chester, PA, USA
Membrane filters 0.2 μM	Pall Corp., Port Washington, NY, USA
Microcentrifuge tube (1.5 mL)	USA Scientific, Orlando, FL, USA
Microcentrifuge tube seal-rite (2.0 mL)	USA Scientific, Orlando, FL, USA
Microcentrifuge tube seal-rite (0.5 mL)	USA Scientific, Orlando, FL, USA
Microplates, 96-well ELISA	Greiner Bio-One GmbH, Germany
Nalgene® syringe filters, polyethersulfone, 25 mm, 0.2 μm	VWR, West Chester, PA, USA
PD-10 column (SephadexTM G-25M; 14.5×50 mm)	GE Healthcare, Uppsala, Sweden
Rainin® pipette tips (10, 250, 1000 μL)	Rainin, Woburn, MA, USA

Tips GelWell 0.57 mm 10 μL GT-10-6	Rainin, Woburn, MA, USA
Weigh paper	VWR, West Chester, PA, USA
Weigh boats	USA Scientific, Orlando, FL, USA

2.2 Purification and partial characterization of ferret trypsin from pancreatic tissue

2.2.1 Sulfuric acid extraction

Ferret pancreata were received frozen and kept in a -20°C freezer until purification. After enough pancreata had been collected, the tissue was removed from the freezer and thawed at room temperature. The tissue was then cut up with a scalpel blade into 1 cm pieces and any fatty tissue was removed. Extraction of proteins was achieved by a standard protocol that was slightly modified to account for the low weight of the ferret pancreata. Briefly, 10 mL of .125 M sulfuric acid was added to a beaker containing one pancreas, regardless of weight. The beaker was quickly placed into a bucket of ice and covered with Parafilm® with one hole in the top. The solution was then homogenized with a tissue grinder until the mixture was smooth and all the tissue had been liquefied. The mixture was poured into a 50 mL centrifuge tube and spun in the centrifuge at 18,000 RCF at 4°C for 45 minutes. The supernatant was carefully decanted and saved for further purification while the pellet was set aside for later evaluation.

2.2.2 Ammonium sulfate precipitation

Ammonium sulfate precipitation was carried out in two steps. For step one a 0.8 M ammonium sulfate was used while 3.0 M ammonium sulfate was used for step two. The supernatant was kept after the first step, while the pellet was retained after the

second step. All fractions were analyzed by SDS-PAGE gel and screened with the tryptic activity assay.

2.2.3 Gel filtration

Gel filtration was done on a Sephacryl S-100 26 x 60 HR with buffer one (200 mM NaCl, 50 nM $CaCl_2$, 0.1 g/L NaN_3, pH 2.6). After the column was equilibrated with buffer one, the pellets from 3.0 M ammonium sulfate precipitation were completely dissolved in 5 mL of the same buffer and then filtered through a 0.2 μM syringe filter. The solution was loaded onto the column with a flow rate of 1 mL/min and 5 mL fractions were collected for analysis and further purification.

2.2.4 Assay for tryptic activity

A 50 μL aliquot was taken from each fraction and the pH was adjusted by the addition of 50 μL of buffer two (1 M Tris-HCl, pH 8.0). Fifty μL of a porcine enterokinase solution (1 mg/mL in buffer two) was added to activate any trypsinogen present. After incubation at 37^0C, all samples plus controls were assayed for tryptic activity using the method described by Schwert and Takenaka [41].

2.2.5 Trypsinogen activation

All fractions that had activity were pooled and the pH was adjusted to 8.0 by adding concentrated NaOH. A solution of 15 mL of buffer two and enterokinase was added to the concentration of 1 mg/mL to begin activation. Starting off by adding approximately 3 mL of the solution it was then left to incubate and the activity was checked every two hours. Every two hours, 50 μL was taken from the pool and screened for tryptic activity. The time of trypsinogen activation varies widely. If the activity did

not increase after 8-10 hours, more of the enterokinase solution was added, and screening was continued every two hours. After the activity had plateaued or slightly decreased, the solution was then applied onto the benzamidine column.

2.2.6 Affinity chromatography and inhibition of trypsin

Affinity chromatography was achieved on a benzamidine sepharose column with a series of buffers to wash off contaminants, elute the purified trypsin, and clean up and regenerate the column. All fractions were collected and pooled, then the pH was adjusted to pH 8.0 using concentrated NaOH. Immediately after pH 8.0 was reached, 2 mL of a 1 mg/ml Na-p-tosyl-ʟ-lysine chloro-methyl ketone (TLCK) solution was added to inhibit trypsin activity. Once again the activity was monitored, and if such activity persisted, more of the TLCK solution was added and the activity was further monitored. The trypsin/TLCK solution was left to incubate at room temperature for 6 hours. The solution was the dialyzed against 4 L of 1 mM HCl for 4 hours, three times (for a total of 12 hours). Afterwards, the trypsin was screened for activity to ensure complete inhibition.

2.2.7 Partial characterization

Pre-cast electrophoresis gels, chamber, power supply, and molecular weight markers (SeeBlue Plus2 and Mark 12) were purchased from Invitrogen, Carlsbad, CA, USA. Manufacturer's instructions were followed with the following parameters: 12% Bis-Tris gels, 200 V constant voltage for 47 minutes. After electrophoresis, the gels were stained with Imperial stain for 45 minutes then destained with H_2O for 2 hours. Finally, gel pictures were taken using Gel Doc™ XR+ System from Bio-Rad Laboratories,

Hercules, CA, USA to determine purity. Finally, the concentration was determined before the final prep and storage (Figure 1). The pure ferret trypsin protein was sent to the Protein Chemistry Laboratory at Texas A&M University for amino acid sequence analysis by Automated Edman Chemistry and to determine sequence homology with trypsin of other species. N-terminal amino acid sequence for the first 6 amino acids was determined.

2.3 Production of anti-ferret trypsin antiserum in rabbits

Two New Zealand White rabbits (*Oryctolagus cuniculus)* were injected with pure ferret trypsin at Lampire Biological Laboratories, Pipersville, Pennsylvania, USA for production of anti-ferret trypsin antiserum. Briefly, each rabbit was injected subcutaneously with 1 mL of a solution consisting of 300 µg of ferret trypsin in 0.5 mL of phosphate buffered saline (PBS) mixed with 0.5 mL complete Freund's adjuvant. Reinoculations with 300 µg of ferret trypsin in 0.5 mL of PBS mixed with 0.5 mL of incomplete Freund's adjuvant were performed 7, 14, 28, 56, and 84 days after initial inoculation in order to boost the immune response to the antigen. Blood samples were collected by venipuncture of the ear vein after the first injection for the pre-bleed and two weeks after each of the last three booster injections for the test bleeds. After a total of 6 injections, both rabbits were exsanguinated and the collected serum was sent to the Gastrointestinal Laboratory at Texas A&M University for the development of a radioimmunoassay (RIA).

2.4 Set-up of a RIA for ferret trypsin-like immunoreactivity

2.4.1 Iodination of ferret trypsin

Titers of anti-ferret trypsin antibodies in the serum of the rabbits were determined using pure ferret trypsin protein radiolabeled with ^{125}I using the chloramine-T method [42]. All buffers for this procedure were prepared fresh, and the iodination procedure was carried out under a fume hood. The bottle containing ^{125}I was kept behind a lead shield within the fume hood.

A miniature stir bar and 10 µL of 0.25 M sodium phosphate buffer (pH 7.5) were placed in a 5 mL polystyrene tube above a stir plate. While stirring, 9 µL of ^{125}I (0.1 mCi/µL at the time of production) was added to the polystyrene reaction tube using a Hamilton syringe. Next, 10 µL of purified ferret trypsin in PBS (1 mg/mL) and 10 µL chloramine-T solution (2 mg/mL chloramine-T in 0.05 M sodium phosphate buffer) were added to the tube. After 45 seconds, 100 µL sodium metabisulfite solution (0.4 mg/mL $Na_2S_2O_5$ in 0.05 M sodium phosphate buffer, pH 7.5) and 860 µL potassium iodide solution (2 mg/mL KI in 0.05 M sodium phosphate buffer, pH 7.5) were added in rapid succession.

To measure the total radioactivity, two 10 µL aliquots of the 1.0 mL mixture were pipetted into separate polystyrene tubes and each diluted with 990 µL of RIA buffer (0.05 M sodium phosphate solution, 0.2 g/L NaN_3, 5 g/L BSA, pH 7.5). Two 10 µL aliquots were taken from this 1.0 mL mixture and pipetted into separate polypropylene tubes labeled TC for “total count” for measurement in the gamma counter (2470 Automatic Gamma Counter Wizard^2®).

A disposable PD-10 desalting column (SephadexTM G-25M; 14.5×50 mm) was equilibrated with 3 column volumes of a concentrated BSA solution (50 mM monobasic sodium phosphate solution and 50 mM dibasic sodium phosphate solution, mixed to achieve a pH of 7.5, with subsequent addition of 5 g/L BSA and 0.2 g sodium azide) to prevent nonspecific protein binding to the dextran resin of the column. The remaining 980 µL of the original solution was poured onto the column in order to separate the iodinated protein from free ^{125}I by size exclusion. The eluent was collected in a polystyrene tube as fraction number 1. Subsequently, 1 mL aliquots of RIA buffer were used as the mobile phase, and 1 mL fractions of eluent were collected in individual polystyrene tubes numbered 2 to 15.

Ten µL of each eluent fraction was transferred to polypropylene tubes, labeled 1 through 15. The two 10 µL aliquots labeled TC were used to determine the total radioactivity and fractions 1 through 15 were measured in the gamma counter and the counts per minute (CPM) were recorded. Using Microsoft Excel to plot the CPM measured values versus the fraction number was used to create a curve with two peaks. The first peak consisted of fractions 4 and 5, and the second peak consisted of fractions 10 to 13, corresponding to the fractions with the highest radioactivity. Since the iodinated protein has a higher molecular weight than free ^{125}I, it elutes earlier and was thus assumed to be contained in fractions 4 and 5.

This iodination procedure was carried out monthly to ensure high specific radioactivity, as ^{125}I has a half-life of 60 days [42]. Fraction 4 had the highest radioactivity of all fractions and was chosen for the production of the tracer. Tracer was

produced as needed and was adjusted to approximately 30,000 CPM per 100 µL tracer by dilution with RIA buffer. Both the final tracer solution and the remainder of fraction 4 were kept at 4°C and discarded with other radioactive materials after 30 days.

2.4.2 Ferret trypsin-like immunoreactivity RIA procedure

Anti-ferret trypsin rabbit antiserum was diluted with RIA buffer to determine the best total binding. The following antibody dilutions were assessed to see which dilution results in the most specific binding: 1:1000, 1:2000, 1:4000, 1:8000, 1:10,000, and 1:20,000. Incubation times of 2, 24, and 48 hours after addition of tracer to the sample tubes were evaluated. As mentioned previously, the tracer was produced from fraction 4 of the iodination and was adjusted to approximately 30,000 CPM per 100 µL. Standards of pure ferret trypsin were made in concentrations of 0.78, 1.56, 3.13, 6.25, 12.5, 25.0, 50.0, 100, and 200 µg/L by serial dilution, and standards were kept at -80°C until needed.

Each RIA procedure was carried out in a radiation room at room temperature (approximately 23°C). Briefly, each ferret serum sample was diluted 1:10 with RIA buffer. Standards were removed from the freezer and 100 µL each were pipetted into two polypropylene tubes. Next, 100 µL of diluted ferret serum samples were aliquoted into two polypropylene tubes before tracer and antiserum were added to all standards and samples.

The tubes labeled TC contained only 100 µL of tracer. The tubes labeled NB contained 200 µL RIA buffer and 100 µL tracer. The tubes labeled B_0 contained 100 µL of RIA buffer, 100 µL tracer, and 100 µL anti-ferret trypsin antibodies. After 100 µL

tracer and 100 μL diluted antiserum were added to all standards and ferret serum samples, all tubes were vortexed and allowed to incubate at room temperature for 24 hrs. After 24 hours, 100 μL of rabbit carrier serum (1 mL of serum from a healthy rabbit in 99 mL of RIAB) and 1 mL of precipitating solution were added to every tube, except TC. Next, the tubes were vortexed and spun in a centrifuge at 3,800 rpm for 30 minutes at 4°C. The polypropylene tubes were promptly removed from the centrifuge and transferred to foam racks. Lastly, the samples were decanted and read with the gamma counter.

2.5 Analytical validation of the ferret trypsin-like immunoreactivity RIA

Excess ferret serum samples from unrelated projects at the Gastrointestinal Laboratory at Texas A&M University were used to analytically validate the assay by determination of dilutional parallelism, spiking recovery, intra-assay variability, and inter-assay variability. Assay sensitivity was assessed by setting up 10 duplicates of B_0 (100 μL anti-ferret trypsin antibodies plus 100 μL RIA buffer) and calculating the mean and standard deviation of the raw counts. The mean counts minus three standard deviations was calculated and the value estimated on the standard curve. The calculated sensitivity was used as the lower limit of detection of the assay.

All ferret serum samples were kept undiluted at -80°C until use and diluted to the standard 1:10 dilution using RIA buffer after thawing the samples at room temperature. Assay linearity was evaluated by assessing dilutional parallelism for 7 different serum samples at serial dilutions of 1:10, 1:20, 1:40, and 1:80 for each sample. The accuracy of the assay was measured by spiking 6 different serum samples with equal volumes of

solutions with known concentrations of ferret trypsin (0.39, 0.78, 1.56, 3.12, 6.25, 12.5, 25, 50 µg/L). The percentage of standard antigen recovery was calculated as the observed-to-expected ratio (O/E%):

O/E% = [observed value (µg/L) / expected value (µg/L)] x 100.

To evaluate the precision of the RIA, 7 different serum samples were analyzed 10 times within the same assay run. The intra-assay coefficient of variation (%CV) was calculated as:

%CV = (standard deviation / mean) x 100.

Assay reproducibility was evaluated by assaying 9 different serum samples in 10 separate assay runs, followed by calculating the inter-assay %CVs. All ferret serum validation samples were run in duplicate fashion and the same 1:8,000 antiserum dilution and a 24 hour incubation time.

2.6 Ferret trypsin-like immunoreactivity RIA reference interval

Healthy ferret serum samples from unrelated projects were used for establishment of a reference interval. Ferrets were determined to be healthy by owner questionnaire. All samples were ran at the standard 1:10 dilution and their concentrations recorded. The reference interval for serum ferret TLI was determined based on the central 95th percentile measured in 35 healthy ferrets with Microsoft Excel freeware add-in reference value advisor V2.1, using the robust Box-Cox transformed data [43].

2.7 Healthy control ferrets vs. ferrets with acute pancreatitis

Dr. John Engelhardt and colleagues from the Anatomy and Cell Biology Department at the University of Iowa Carver College of Medicine had previously

conducted experiments to induce acute pancreatitis (AP) in ferrets. Three ferrets were hyperstimulated with caerulein to induce AP and four ferrets were used as healthy controls (HC). Control ferrets were kept in the same environment and fed the same diet as AP ferrets. Serum obtained from all 7 ferrets used in this study was collected and shipped to the Gastrointestinal Laboratory at Texas A&M University and kept at -80°C until analysis by the mTLI RIA. Ferret serum not sent to Texas A&M University was used to determine serum lipase activities (IU/L) at University of Iowa Carver College of Medicine. After analytical validation of the mTLI assay, the 7 ferret serum samples (3 AP, 4 HC) were analyzed at the standard 1:10 dilution. A Pearson correlation coefficient was calculated between the two variables of lipase activity and mTLI concentration using GraphPad Prism V7.0 for Windows, GraphPad Software, La Jolla, California USA.

3. RESULTS

3.1 Purification and partial characterization of ferret trypsin

Trypsin was successfully purified from ferret pancreatic tissue. After adding 10 mL of 0.125 M sulfuric acid to one minced ferret pancreas and after homogenizing the solution with a tissue grinder, the solution was centrifuged. This procedure yielded about 9.5 mL of supernatant that was kept for further purification. A two-step ammonium sulfate precipitation with increasing concentrations of ammonium sulfate produced two solutions with a pellet and a supernatant. The supernatant was kept after the first precipitation, while the pellet was kept after the second precipitation step. The pellet from the ammonium precipitation was loaded onto a gel filtration column, resulting in a peak after approximately 50-60 mL of buffer was applied. The fractions that contained the peak were saved for tryptic activity screening and SDS-PAGE analysis. Tryptic activity between purification steps was measured as described previously by Schwert and Takenaka [41]. After pooling all fractions with tryptic activity and adjusting the pH to 8.0, trypsinogen was activated by addition of an enterokinase solution. After activity reached a maximum plateau, the solution was applied to a benzamidine column. Affinity chromatography with a benzamidine column led to a single peak (Figure 1) that contained purified trypsin eluting after addition of elution buffer (50 mM Sodium acetate, 2 mM $CaCl_2$, pH 3.25). After adjusting the pH to 8.0, 2 mL of a 1 mg/ml Na-p-tosyl-L-lysine chloro-methyl ketone (TLCK) solution was added to inhibit trypsin activity for storage at -20°C.

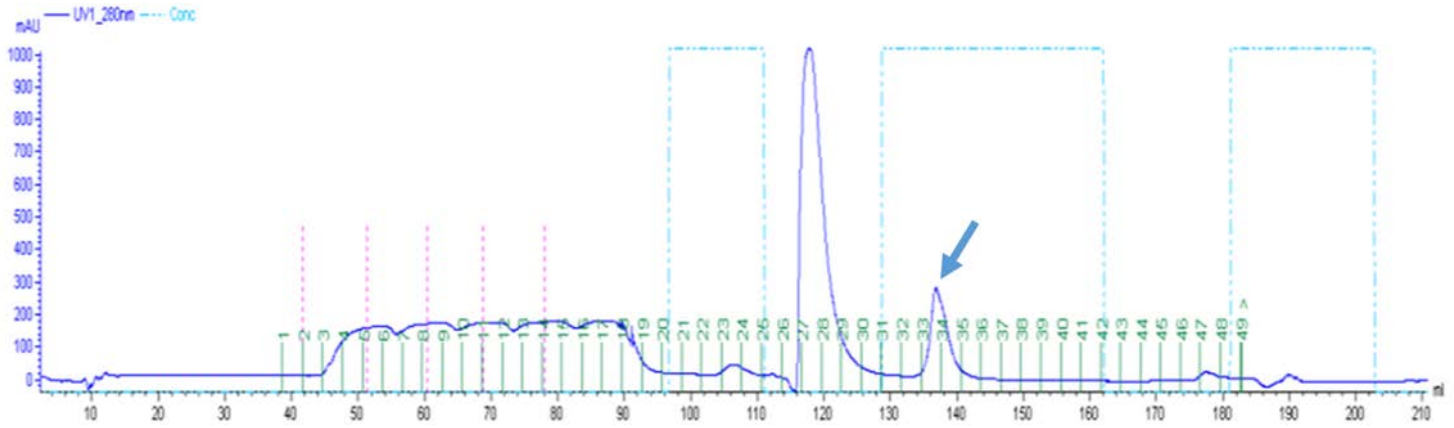

Figure 1. Affinity chromatography of partially purified ferret trypsin. This figures shows a representative chromatogram of affinity chromatography on a benzamidine column. The dark blue line shows the absorbance at a wavelength of 280 nm during chromatography. The green numbers represent the fractions. The pink dotted lines indicate injection of protein onto the column. The light blue line shows the concentration (%) of elution buffer. The peak indicated by the arrow represents pure ferret trypsin.

The molecular weight of ferret trypsin was estimated by SDS-PAGE stained with Coomassie blue stain to be between 22-25 kDa (Figure 2). The amino acid sequence of the first six amino acids of the mature end of the trypsin was determined to be: I-V-G-G-X-T (X is an unknown amino acid). The amino acid sequence was determined to be highly homologous to trypsin from several other species (Figure 3) according to the sequence analysis report provided by the Protein Chemistry Laboratory at Texas A&M University.

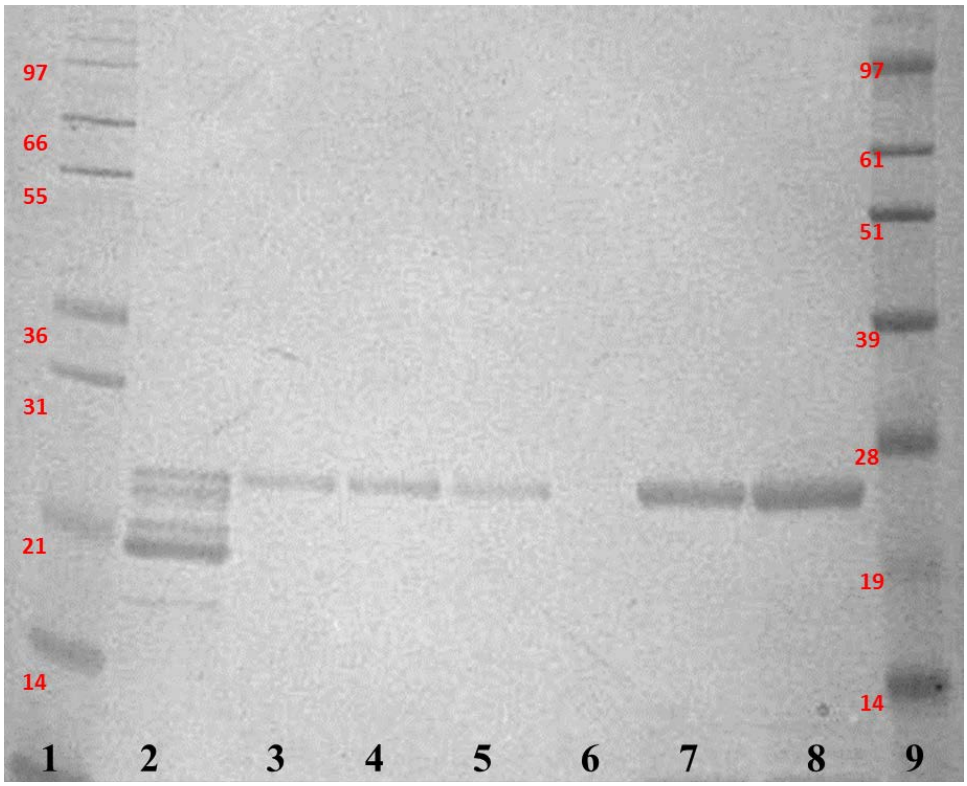

Figure 2. SDS-PAGE gel analysis of fractions after affinity chromatography. Lanes 1 and 9 are molecular weight markers with weights (kDa) in red. Lane 2 is an aliquot of partially purified ferret trypsin before affinity chromatography. Lanes 3 through 8 are the five fractions with tryptic activity taken from affinity chromatography. The single band in lanes 3, 4, 5, 7, and 8 represent pure ferret trypsin.

Species	Trypsin-like Sequence					
Human	I	V	G	G	Y	T
Pig	I	V	G	G	Y	T
Rat	I	V	G	G	Y	T
Cat	I	V	G	G	Y	T
Dog	I	V	G	G	Y	T

Figure 3. Sequence homology. This figure shows the N-terminal amino acid sequence of trypsinogen from different mammalian species using the one letter amino acid code: human trypsinogen 1 and 3, anionic and cationic porcine trypsinogen, rat trypsinogen 1 and 2, feline trypsinogen, canine anionic trypsinogen, and ferret trypsin-like protein [44,45,46,47,48].

3.2 Production of anti-ferret trypsin antiserum in rabbits

Serum anti-ferret trypsin antibody titers were evaluated in both rabbits after inoculation. After the last inoculation, the antibody titers at different dilutions were determined by RIA (Figures 4a & 4b). Titers from both rabbits were sufficient for RIA development.

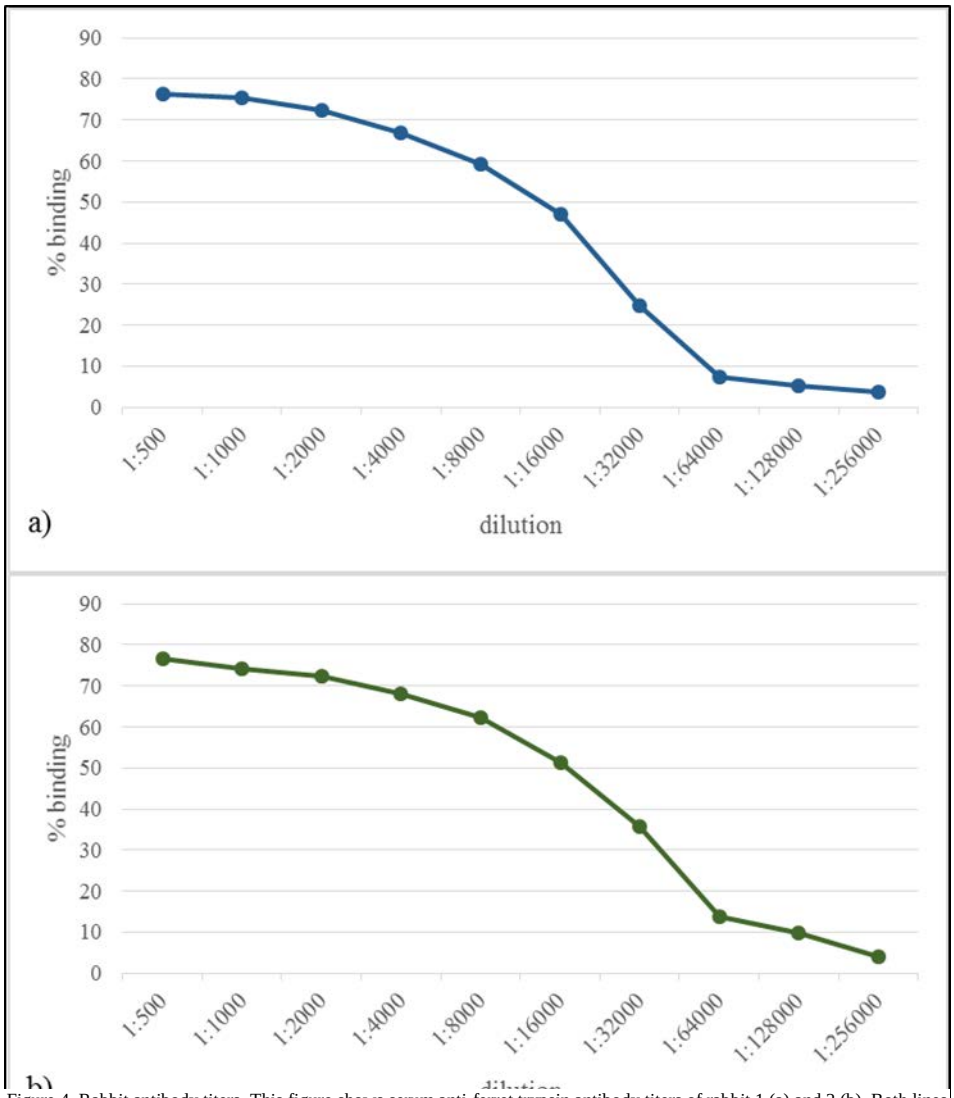

Figure 4. Rabbit antibody titers. This figure shows serum anti-ferret trypsin antibody titers of rabbit 1 (a) and 2 (b). Both lines represent the serum collected after the final inoculation. The figure displays % binding, as determined by RIA, at different dilutions (from 1:500 to 1:256,000).

3.3 Development and analytical validation of a RIA for ferret trypsin-like immunoreactivity

Monthly iodination procedures were carried out to ensure quality binding, as ^{125}I is known to have a half-life of 60 days [42]. Fraction 4 from the iodination procedure was used for the production of tracer and adjusted to 30,000 CPM per 100 μL for each radioimmunoassay (RIA). Every RIA experiment used the same 1:8,000 antibody dilution from rabbit 1 and 24 hour incubation after addition of tracer.

A representative standard curve for the ferret trypsin-like immunoreactivity RIA is shown in Figure 5. Observed-to-expected ratios for dilutional parallelism for the 7 serum samples tested ranged from 95.2% to 119.4% (mean ± standard deviation [s], 105.7% ± 8.5%) (Table 1). Observed-to-expected ratios for spiking recovery for the 6 serum samples assayed ranged from 94.5% to 113.0% (mean ± [s], 103.9% ± 7.2%) (Table 2). Coefficients of variation for intra-assay variability for the 7 serum samples analyzed were 4.1%, 3.5%, 5.3%, 5.7%, 4.3%, 3.5%, and 2.7% (Table 3). Also, coefficients of variation for inter-assay variability for the 9 serum samples tested were 7.3%, 6.4%, 4.2%, 3.5%, 5.2%, 5.4%, 5.1%, 7.5%, and 8.2% (Table 4). The sensitivity of the assay was calculated to be 0.55 μg/L. The healthy reference interval (n = 35) was determined to be 17.7 to 123.2 μg/L.

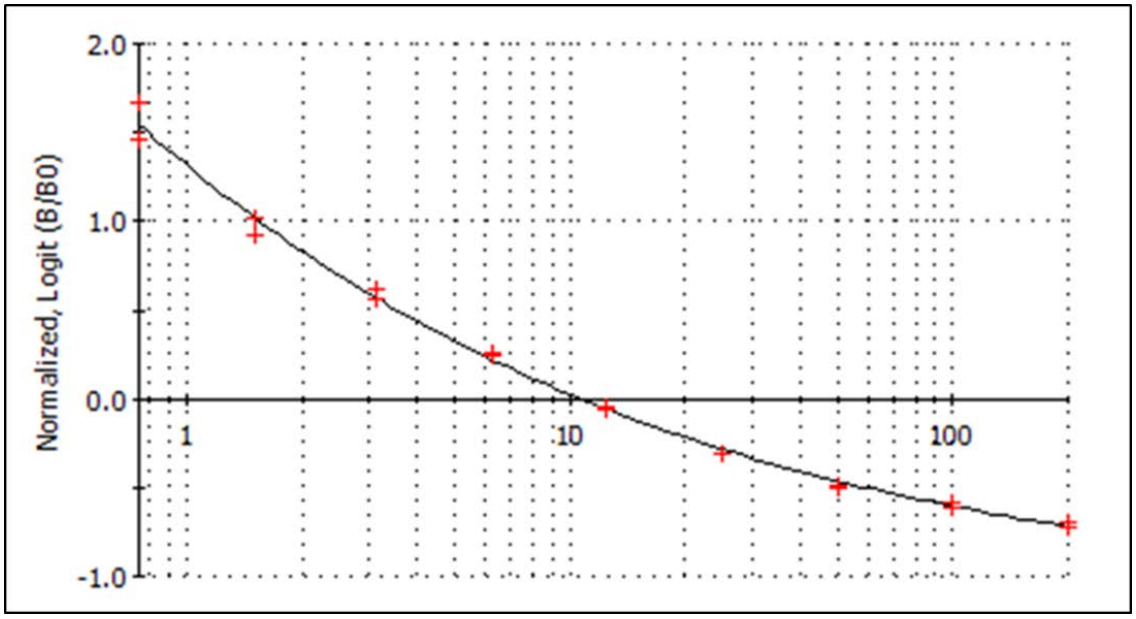

Figure 5. mTLI RIA standard curve. This figure shows one representative standard curve for the mTLI RIA. Standards are marked with red plus signs. Concentrations of standards are marked on the x-axis in logarithmic form. $\%B/B_0$ values are on the y-axis and are calculated using a normalized four parameter fit equation.

Table 1. Dilutional parallelism of 7 ferret serum samples

Dilution	Observed (µg/L)	Expected (µg/L)	O/E(%)
1:10	153.5		
1:20	90.3	76.8	**117.7**
1:40	46.5	38.4	**121.2**
1:80	27.8	19.2	**144.9**
			119.4

Dilution	Observed (µg/L)	Expected (µg/L)	O/E(%)
1:10	8.0		
1:20	4.0	4.0	**101.1**
1:40	2.0	2.0	**100.4**
1:80	0.6	1.0	**61.8**
			100.8

Dilution	Observed (µg/L)	Expected (µg/L)	O/E(%)
1:10	128.6		
1:20	64.9	64.3	**100.9**
1:40	33.3	32.2	**103.6**
1:80	20.1	16.1	**125.0**
			102.3

Dilution	Observed (µg/L)	Expected (µg/L)	O/E(%)
1:10	7.0		
1:20	3.6	3.5	**104.7**
1:40	1.7	1.7	**98.6**
1:80	1.0	0.9	**111.2**
			101.7

Dilution	Observed (µg/L)	Expected (µg/L)	O/E(%)
1:10	76.9		
1:20	39.6	38.5	**103.0**
1:40	16.8	19.2	**87.4**
1:80	7.7	9.6	**80.1**
			95.2

Dilution	Observed (µg/L)	Expected (µg/L)	O/E(%)
1:10	3.5		
1:20	2.0	1.8	**117.0**
1:40	1.0	0.9	**112.2**
1:80	0.5	0.4	**121.2**
			114.6

Dilution	Observed (µg/L)	Expected (µg/L)	O/E(%)
1:10	13.9		
1:20	7.2	7.0	**103.4**
1:40	3.8	3.5	**108.7**
1:80	1.8	1.7	**104.1**
			106.0

Min	**95.2**
Max	**119.4**
Mean	**105.7**
SD	**8.5**

Table 1. This table shows the serial dilution of 7 serum samples throughout the working range. Observed-to-expected ratios are in bold and the minimum, maximum, mean, and standard deviation of those 7 observed-to-expected ratios is provided in the box.

Table 2. Spiking recovery of 6 ferret serum samples

Concentation added (µg/L)	Observed (µg/L)	Expected (µg/L)	O/E (%)
0	2.1		
0.39	2.0	2.4	**81.0**
0.78	2.6	2.8	**91.9**
1.56	3.8	3.6	**105.3**
3.13	5.0	5.2	**96.1**
6.25	8.6	8.3	**103.2**
12.5	9.1	14.6	**62.8**
25	32.0	27.1	**118.2**
50	59.0	52.1	**113.2**
Mean			**96.5**
SD			**18.0**

Concentation added (µg/L)	Observed (µg/L)	Expected (µg/L)	O/E (%)
0	4.2		
0.39	3.8	4.6	**83.1**
0.78	4.9	4.9	**98.8**
1.56	5.9	5.8	**103.2**
3.13	7.4	7.3	**100.9**
6.25	10.8	10.4	**103.8**
12.5	17.6	16.7	**105.6**
25	35.9	29.2	**123.0**
50	81.4	54.2	**150.3**
Mean			**108.6**
SD			**20.0**

Concentation added (µg/L)	Observed (µg/L)	Expected (µg/L)	O/E (%)
0	3.8		
0.39	3.4	4.2	**82.5**
0.78	4.0	4.6	**88.6**
1.56	5.2	5.3	**97.2**
3.13	7.0	6.9	**100.8**
6.25	10.2	10.0	**101.4**
12.5	9.9	16.3	**60.7**
25	32.9	28.8	**114.2**
50	59.6	53.8	**110.8**
Mean			**94.5**
SD			**17.2**

Concentation added (µg/L)	Observed (µg/L)	Expected (µg/L)	O/E (%)
0	6.4		
0.39	5.6	6.7	**82.7**
0.78	7.7	7.1	**108.0**
1.56	8.0	7.9	**101.1**
3.13	9.1	9.5	**95.5**
6.25	13.3	12.6	**105.2**
12.5	22.5	18.9	**119.2**
25	32.6	31.4	**104.0**
50	77.0	56.4	**136.6**
Mean			**106.6**
SD			**16.0**

Concentation added (µg/L)	Observed (µg/L)	Expected (µg/L)	O/E (%)
0	3.9		
0.39	4.1	4.3	**94.4**
0.78	5.0	4.7	**107.8**
1.56	6.0	5.5	**108.5**
3.13	7.1	7.1	**100.7**
6.25	10.0	10.2	**98.7**
12.5	15.9	16.4	**96.7**
25	29.8	28.9	**103.0**
50	66.4	53.9	**123.2**
Mean			**104.1**
SD			**9.2**

Concentation added (µg/L)	Observed (µg/L)	Expected (µg/L)	O/E (%)
0	9.4		
0.39	9.7	9.7	**99.7**
0.78	11.2	10.1	**110.9**
1.56	12.4	10.9	**113.5**
3.13	15.1	12.5	**120.6**
6.25	18.3	15.6	**117.0**
12.5	24.7	21.9	**113.0**
25	37.6	34.4	**109.3**
50	71.4	59.4	**120.2**
Mean			**113.0**
SD			**6.8**

Min	**94.5**
Max	**113.0**
Mean	**103.9**
SD	**7.2**

Table 2. This table shows data from spiking recovery of 6 serum samples in the lower and middle regions of the working range. Observed-to-expected ratios are in bold and the minimum, maximum, mean, and standard deviation of those 6 observed-to-expected ratios is provided in the box.

Table 3. Intra-assay variabililty of 7 ferret serum samples							
Sample	**1**	**2**	**3**	**4**	**5**	**6**	**7**
Number of repeats	10	10	10	10	10	10	10
Mean (µg/L)	15.8	12.4	7.9	7.5	7.4	6.3	3.5
Standard deviation (µg/L)	0.6	0.4	0.4	0.4	0.3	0.2	0.1
% CV	**4.1**	**3.5**	**5.3**	**5.7**	**4.3**	**3.5**	**2.7**

Table 3. This table shows the results of intra-assay variability of the mTLI RIA for 7 different serum samples, from highest to lowest concentration. Coefficients of variation (%CV) are shown in bold.

Table 4. Inter-assay variabililty of 9 ferret serum samples									
Sample	**1**	**2**	**3**	**4**	**5**	**6**	**7**	**8**	**9**
Number of repeats	10	10	10	10	10	10	10	10	10
Mean (µg/L)	20.1	14.5	10.4	8.1	7.3	6.9	6.2	4.9	3.7
Standard deviation (µg/L)	1.5	0.9	0.4	0.3	0.4	0.4	0.3	0.4	0.3
% CV	**7.3**	**6.4**	**4.2**	**3.5**	**5.2**	**5.4**	**5.1**	**7.5**	**8.2**

Table 4. This table shows the results of inter-assay variability of the mTLI RIA for 9 different serum samples, from highest to lowest concentration. Coefficients of variation (%CV) are shown in bold.

3.4 Healthy control ferrets vs. ferrets with acute pancreatitis

Serum total lipase activity in ferret serum was analyzed at the University of Iowa Carver College of Medicine. The serum total lipase activities for control ferrets were 112.5, 75.9, 119.2, and 86.0 IU/L while AP ferrets had activities of 144.6, 276.9, and 334.2 IU/L. In the serum from the same ferrets sent to the Gastrointestinal Laboratory, the four control ferrets had trypsin-like immunoreactivity (mTLI) RIA concentrations of 23.0, 24.0, 24.5, and 25.3 µg/L, and the three ferrets with experimentally induced acute pancreatitis had mTLI concentrations of 62.8, 76.2, and 143.6 µg/L. These two biomarkers correlated well (Pearson r = 0.70), as shown in Figure 6.

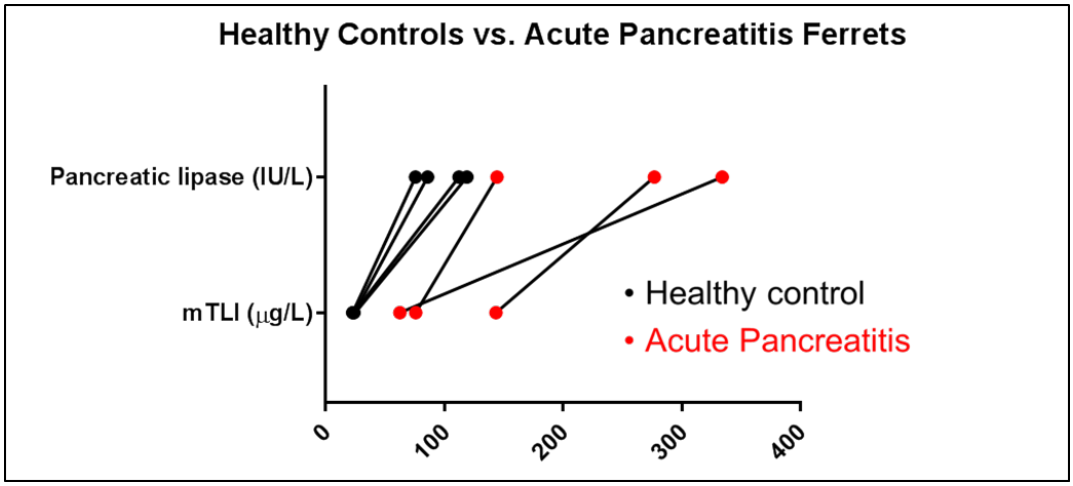

Figure 6. Healthy controls vs. acute pancreatitis ferrets. Correlation between serum total lipase activity (IU/L) and serum mTLI concentration (μg/L) for healthy control ferrets (black dots) and ferrets with acute pancreatitis (red dots). The calculated Pearson correlation coefficient, r, was 0.70. All acute pancreatitis ferrets had higher total serum total lipase activities and mTLI concentrations than healthy controls.

4. DISCUSSION

4.1 Purification and partial characterization of ferret trypsin

This is the first report of the purification of ferret trypsin from pancreatic tissue. The purification procedure followed modified versions of trypsin purification procedures reported for other species [47,49]. The assay for tryptic activity was performed along with SDS-PAGE analysis to determine which aliquots should be used for the next steps of purification.

Sulfuric acid extraction and ammonium sulfate precipitation are widely used purification methods [50]. Gel filtration chromatography is a traditional separation technique where larger molecules elute before smaller molecules, separating proteins by molecular size [51]. Affinity chromatography is another widely used method for protein purification. In general, a ligand molecule binds to the molecule of interest and is immobilized. Contaminating molecules are eluted by washing the column with different buffers with different properties (pH, NaCl concentration, etc.) until the molecule of interest is ready to be eluted [52,53].

After the final affinity chromatography purification step, the purified material showed a single band on SDS-PAGE when stained with Coomassie blue stain (Figure 2). The molecular weight of ferret trypsin was estimated to between 22-25 kDa, similar to trypsins and trypsinogens from other species. For example, canine cationic trypsin is reported to have a molecular mass of 23.8 kDa and feline trypsinogen and feline trypsin are reported to have a molecular mass of 22.6 kDa and 21.0 kDa, respectively [48,47].

The N-terminal amino acid sequence of ferret trypsin was homologous to that of trypsin in other species (Figure 3). Ferret trypsin may have a modified amino acid in position 5 that cannot be identified by the standard procedures of Edman degradation.

4.2 Production of anti-ferret trypsin antiserum in rabbits

Pure ferret trypsin was sent to Lampire Biological Laboratories, Pipersville, Pennsylvania, USA for production of anti-ferret trypsin antiserum in rabbits. The vaccination protocol was slightly modified from their standard antibody production protocol, adding another inoculation to ensure high antibody titers. Both rabbits had an adequate immune response (Figures 4a & 4b). In conclusion, anti-ferret trypsin antiserum was successfully raised in two New Zealand White rabbits. Aliquots from both rabbits were used in the development of the mTLI RIA.

4.3 Development and analytical validation of a RIA for ferret trypsin-like immunoreactivity

A radioimmunoassay (RIA) for the measurement of ferret trypsin-like immunoreactivity (mTLI) in serum was successfully established. There are no standardized cut-off values for observed-to-expected ratios for dilutional parallelism or spiking recovery nor for coefficients of variation for intra-assay and inter-assay variability. In our laboratory, acceptable observed-to-expected ratios are considered to range from 80% to 120%, and acceptable coefficients of variation are under 10% to 15%. Observed-to-expected ratios for serial dilution were between 95.2% and 119.4%, which suggests the assay is sufficiently linear (Table 1). Observed-to-expected ratios for spiking recovery ranged from 94.5 to 113.0%, which suggests the assay is accurate

(Table 2). Coefficients of variation for intra-assay variability were all less than 6.0%, which suggest that the assay is sufficiently precise (Table 3). Also, coefficients of variation for inter-assay variability were all less than 9.0%, which suggests that the assay is reproducible (Table 4).

The reference interval for mTLI (n = 35) was determined to be 17.7 to 123.2 µg/L. This assay has a working range of 0.55 to 200 µg/L, as defined by the lower limit of detection and the highest standard concentration, and the healthy reference interval is well within that range.

In summary, the mTLI RIA described here was sufficiently sensitive, linear, accurate, and reproducible for use.

4.4 Healthy control ferrets vs. ferrets with acute pancreatitis

Samples from a small study at University of Iowa Carver College of Medicine consisted of three ferrets induced to have acute pancreatitis and four healthy control ferrets were used to demonstrate the biological relevance of the mTLI RIA described. Serum total lipase activity in ferret serum was measured at the University of Iowa Carver College of Medicine. Serum total lipase activity and mTLI concentrations correlated well, with a calculated Pearson correlation coefficient, r, of 0.70 (Figure 6). However, no other statistical analysis was performed as the small sample size provided little statistical power. Further assessment of mTLI in ferrets with AP and CF is therefore needed.

4.5 Limitations

Although the major goal of developing and analytically validating a radioimmunoassay for the measurement of trypsin-like immunoreactivity in ferret serum was accomplished, the study was not without limitations. During the purification, the methods used were carried out with cost-effectiveness in mind. Only the first 6 amino acids of the N-terminal end were determined to save cost. However, the sequence identified is homologous to trypsin from other species [44,45,46,47,48] so the author is confident that the protein purified was ferret trypsin/trypsinogen.

Another limitation was the ferret serum samples used for RIA validation and construction of a reference interval in this study had been collected for unrelated projects conducted at the Gastrointestinal Laboratory at Texas A&M University between 2008 and 2010. At that time, ferret serum samples were collected and logged, accompanied by owner questionnaires that categorized the ferret as either healthy or diseased. Serum samples had remained frozen at -80°C since 2010. Therefore, degradation of serum sample quality could have affected our results, potentially resulting in a falsely lowered reference interval.

The sample size of healthy ferret samples (n = 35) may be considered small, and these ferrets were only determined healthy based on owner questionnaires. However, this may be overcome with studies that provide their own healthy controls, allowing direct comparison of healthy and diseased groups. For example, the three acute pancreatitis ferret serum samples had mTLI concentrations that were at least twice as high as those of the four healthy controls from the same experiment.

The ferret serum samples provided by the University of Iowa Carver College of Medicine demonstrated that the mTLI concentrations of AP ferrets are higher than those of healthy ferrets. However, another limitation was the small sample size providing limited statistical power when comparing the two groups. Future studies of ferrets with induced pancreatitis are being conducted, and plans have been made to have serum harvested and sent to the Gastrointestinal Laboratory at Texas A&M University for mTLI analysis.

Lastly, although ferrets serve as an established animal model for CF [30], we did not assay any serum samples from CF ferrets. We would expect serum mTLI concentrations of adult CF ferrets to be much lower than those of healthy controls, due to pancreatic acinar cell destruction. A logical next step would be to measure serum mTLI from CFTR-knockout ferrets and healthy control ferrets.

5. CONCLUSIONS

The major objective of this project, to develop and analytically validate a radioimmunoassay for the measurement of ferret trypsin-like immunoreactivity (mTLI), was successfully accomplished. In order to develop the mTLI radioimmunoassay (RIA), ferret trypsin had to be purified and antiserum against this protein was raised in rabbits. Then the RIA was developed and analytically validated, a reference interval for healthy ferrets was established, and a small study with four clinically healthy ferrets and three ferrets with induced acute pancreatitis (AP) was conducted.

Ferret trypsin was purified from pancreatic tissue using slightly modified protocols described previously [47,49,52,53]. Partial characterization consisted of SDS-PAGE analysis of ferret trypsin that estimated the molecular mass to be between 22-25 kDa, and the N-terminal amino acid sequence of the first 6 amino acids was homologous to sequences reported for trypsins from other species (Figure 3) [44,45,46,47,48]. After purification, the first step toward immunoassay development was the production of antiserum directed against ferret trypsin raised in New Zealand White rabbits by repeated inoculations of solutions containing a mixture of ferret trypsin and complete or incomplete Freund's adjuvant. Antiserum titers from both rabbits were used in the establishment of the mTLI RIA.

We developed and analytically validated an in-house RIA for the measurement of mTLI that is analytically sensitive, accurate, precise, reproducible, and sufficiently linear for the measurement of TLI in serum samples from ferrets. The working range of the

assay was 0.55 to 200 μg/L. A reference interval for the mTLI RIA was established, although the sample size may be considered small (n = 35).

A small pilot study conducted at the University of Iowa Carver College of Medicine evaluated serum mTLI concentrations in three ferrets with induced pancreatitis and four healthy control ferrets. Serum lipase activities were measured by Dr. Engelhardt and colleagues at the University of Iowa Carver College of Medicine and those results were sent along with leftover ferret serum for analysis of serum mTLI RIA concentrations. We demonstrated that the mTLI concentrations of AP ferrets are higher than the mTLI concentrations of healthy ferrets in this small pilot study. These findings correlated with those for serum lipase activity with a Spearman r = 0.70 (Figure 6). Correlation between these two assays suggests that mTLI concentration may be a useful marker for exocrine pancreatic function during AP.

In conclusion, further studies are needed to determine if the mTLI RIA is useful in evaluating both spontaneous and experimental exocrine pancreatic disorders in ferrets. CF and pancreatitis are two conditions for which researchers have the option for using several different animal models, and each animal model has its strengths and weaknesses. This will allow researchers to use their similarities and differences to better understand life-threatening diseases and to develop life-saving modalities. Both models may benefit using a minimally invasive marker, such as mTLI, to assess exocrine pancreatic function.

REFERENCES

1. Travis J, Roberts RC. Human trypsin. Isolation and physical-chemical characterization. Biochemistry 1969;8:2884-2889.
2. Geokas MC, Largman C, Brodrick JW, Johnson JH. Determination of human pancreatic cationic trypsinogen in serum by radioimmunoassay. American Journal of Physiology: Gastrointestinal & Liver Physiology 1979;236:E77.
3. Steiner JM, Williams DA. Serum feline trypsin-like immunoreactivity in cats with exocrine pancreatic insufficiency. Journal of Veterinary Internal Medicine 2000;14:627-629.
4. Sarles J, Giorgi R, Berthézène P, Munck A, Cheillan D, et al. Neonatal screening for cystic fibrosis: comparing the performances of IRT/DNA and IRT/PAP. Journal of Cystic Fibrosis 2014;13:384-390.
5. Williams DA, Batt RM. Sensitivity and specificity of radioimmunoassay of serum trypsin-like immunoreactivity for the diagnosis of canine exocrine pancreatic insufficiency. Journal of the American Veterinary Medical Association 1988;192:195-201.
6. Steiner JM, Medinger TL, Williams DA. Development and validation of a radioimmunoassay for feline trypsin-like immunoreactivity. American Journal of Veterinary Research 1996;57:1417-1420.
7. Grulke, S. Equine trypsin: purification and development of a radio-immunoassay. Veterinary Research 2003;34:317-330.

8. Yan Z, Stewart ZA, Sinn PL, Olsen JC, Hu J, McCray PB, Engelhardt JF. Ferret and pig models of cystic fibrosis: prospects and promise for gene therapy. Human Gene Therapy Clinical Development 2014;26:38-49.
9. Cutting GR. Cystic fibrosis genetics: from molecular understanding to clinical application. Nature Reviews Genetics 2015;16:45-56.
10. Elborn JS. Cystic fibrosis. The Lancet 2016: DOI: http://dx.doi.org/10.1016/S0140-6736(16)00576-6.
11. Montgomery GS, Howenstine M. Cystic fibrosis. Pediatric Review 2009;30:302-309.
12. O'Sullivan BP, Freedman SD. Cystic fibrosis. The Lancet 2009;373:1891-1904.
13. Stallings VA, Stark LJ, Robinson KA, Feranchak AP, Quinton H. Evidence-based practice recommendations for nutrition-related management of children and adults with cystic fibrosis and pancreatic insufficiency: results of a systematic review. Journal of the American Dietetic Association 2008;108:832-839.
14. Gibson-Corley KN, Meyerholz DK, Engelhardt JF. Pancreatic pathophysiology in cystic fibrosis. The Journal of Pathology 2016;238:311-320.
15. Morrell MR, Pilewski JM. Lung transplantation for cystic fibrosis. Clinics in Chest Medicine 2016;37:127-138.
16. Yusen RD, Edwards LB, Dipchand AI, Goldfarb SB, Kucheryavaya AY, et al. Registry of the International Society for Heart and Lung Transplantation: thirty-third adult lung and heart-lung transplant report; focus theme: primary diagnostic

indications for transplant. The Journal of Heart and Lung Transplantation 2016;35:1158-1169.

17. Wilschanski M, Novak I. The cystic fibrosis of exocrine pancreas. Cold Spring Harbor Perspectives in Medicine 2013;3:1-17.
18. Murphy AJ, Buntain HM, Wainwright CE, Davies PS. The nutritional status of children with cystic fibrosis. British Journal Nutrition 2006;95:321-324.
19. Andersen DH. Cystic fibrosis of the pancreas and its relation to celiac disease: a clinical and pathologic study. American Journal of Diseases of Children 1938;56:344-399.
20. Kerem B, Rommens JM, Buchanan JA, Markiewicz D, Cox TK, et al. Identification of the cystic fibrosis gene: genetic analysis. Science 1989;245:1073-1080.
21. Wilschanski M, Durie PR. Patterns of GI disease in adulthood associated with mutations in the CFTR gene. Gut 2007;56:1153-1163.
22. Wang Y, Wrennall JA, Cai Z, Li H, Sheppard DN. Understanding how cystic fibrosis mutations disrupt CFTR function: from single molecules to animal models. International Journal of Biochemistry and Cell Biology 2014;52:47-57.
23. Sabharwal S. Gastrointestinal manifestations of cystic fibrosis. Journal of Gastroenterology and Hepatology 2016;12:43-47.
24. Durno C, Corey M, Zielenski J, Tullis E, Tsui LC, Durie P. Genotype and phenotype correlations in patients with cystic fibrosis and pancreatitis. Gastroenterology 2002;123:1857-1864.

25. Olivier AK, Gibson-Corley KN, Meyerholz DK. Animal models of gastrointestinal and liver diseases. Animal models of cystic fibrosis: gastrointestinal, pancreatic, and hepatobiliary disease and pathophysiology. American Journal of Physiology - Gastrointestinal and Liver Physiology 2015;308:G459-G471.
26. Navis A, Bagnat M. Loss of CFTR function leads to pancreatic destruction in larval zebrafish. Developmental Biology 2015;399:237-248.
27. Stoltz DA, Rokhlina T, Ernst SE, Pezzulo AA, Ostedgaard LS, et al. Intestinal CFTR expression alleviates meconium ileus in cystic fibrosis pigs. Journal of Clinical Investigation 2013;123:2685-2693.
28. Scholte BJ, Davidson DJ, Wilke M, de Jonge HR. Animal models of cystic fibrosis. Journal of Cystic Fibrosis 2004;3:183-190.
29. Lavelle GM, White MM, Browne N, McElvaney NG, Reeves EP. Animal models of cystic fibrosis pathology: phenotypic parallels and divergences. BioMed Research International 2016;2016:1-14.
30. Chu YK, Ali GD, Jia F, Li Q, Kelvin D, et al. The SARS-CoV ferret model in an infection-challenge study. Virology 2008;374:151-163.
31. Belser JA, Katz JM, Tumpey TM. The ferret as a model organism to study influenza A virus infection. Disease Models & Mechanisms 2011;4:575-579.
32. Sun X, Olivier AK, Yi Y, Pope CE, Hayden HS, et al. Gastrointestinal pathology in juvenile and adult CFTR-knockout ferrets. The American Journal of Pathology 2014;184:1309-1322.

33. Baker SS, Borowitz D, Duffy L, Fitzpatrick L, Gyamfi J, Baker RD. Pancreatic enzyme therapy and clinical outcomes in patients with cystic fibrosis. Journal of Pediatrics 2005;146:189-193.
34. Hue Su K, Cuthbertson C, Christophi C. Review of experimental animal models of acute pancreatitis. HPB: Official Journal of the International Hepato Pancreato Biliary Association 2006;8:264-286.
35. Majumder S, Chari ST. Chronic pancreatitis. The Lancet 2016;387:1957-1966.
36. Granger J, Remick D. Acute pancreatitis: models, markers, and mediators. Shock 2005;24:45-51.
37. Lankisch PG, Apte M, Banks PA. Acute pancreatitis. The Lancet 2015;386:85-96.
38. Pandol SJ, Saluja AK, Imrie CW, Banks PA. Acute pancreatitis: bench to the bedside. Gastroenterology 2007;132:1127-1151.
39. Ruben DS, Scorpio DG, Gabrielson KL, Simon BW, Buscaglia JM. Refinement of canine pancreatitis model: inducing pancreatitis by using endoscopic retrograde cholangiopancreatography. Comparative Medicine 2009;59:78-82.
40. Hunter WM, Greenwood FC. Preparation of iodine-131 labelled human growth hormone of high specific activity. Nature 1962;194:495-496.
41. Schwert GW, Takenaka Y. A spectrophotometric determination of trypsin and chymotrypsin. Biochimica et Biophysica Acta 1955;16:570-575.
42. Bailey GS. The chloramine T method for radiolabeling protein. The Protein Protocols Handbook. Walker JM. Totowa, NJ, Humana Press: 2002;963-965.

43. Geffre A, Concordet D, Braun JP, Trumel C. Reference Value Advisor: a new freeware set of macroinstructions to calculate reference intervals with Microsoft Excel. Veterinary Clinical Pathology 2011;40:107-112.

44. Figarella C, Negri GA, Guy O. The two human trypsinogens. Inhibition spectra of the two human trypsins derived from their purified zymogens. European Journal of Biochemistry 1975;53:457-463.

45. Louvard MN. On bovine and porcine anionic trypsinogens. Biochimica et biophysica acta 1974;371:177-185.

46. MacDonald RJ. Two similar but non-allelic rat pancreatic trypsinogens. Nucleotide sequences of the cloned cDNAs. Journal of Biological Chemistry 1982;257:9724-9732.

47. Steiner JM, Medinger TL, Williams DA. Purification and partial characterization of feline trypsin. Comparative Biochemistry and Physiology - Part B: Biochemistry & Molecular Biology 1997;116:87-93.

48. Pinsky SD. Differential regulation of trypsinogen mRNA translation: full-length mRNA sequences encoding two oppositely charged trypsinogen isoenzymes in the dog pancreas. Molecular and Cellular Biology 1985;5:2669-2676.

49. Williams DA, Batt RM, Beynon RJ. A simple procedure for the purification of the zymogens and active forms of canine anionic trypsin, cationic trypsin and chymotrypsin. Biochemical Society Transactions 1983;11:351-351.

50. Wood WI. Tables for the preparation of ammonium sulfate solutions. Analytical Biochemistry 1976;73:250-257.

51. Laurent TC. A theory of gel filtration and its experimental verification. Journal of Chromatography 1964;14:317-330.

52. Hixson HF. Affinity chromatography of bovine trypsin and thrombin. Methods in Enzymology 1974;34:440-448.

53. Temler RS, Kagi JH. Isolation of human trypsin by affinity chromatography. Enzyme 1977;22:249-255.